AGU PUBLICATIONS

Geophysical Research Letters

RESEARCH LETTER
10.1002/2015GL065345

Key Points:
- Estimation of crustal reflectivity from 750 single-station autocorrelograms
- Moho extraction from 160 station stacks guided by prior information
- Improved Moho surface definition across southeast Australia

Supporting Information:
- Supporting Information S1

Correspondence to:
B. L. N. Kennett,
Brian.Kennett@anu.edu.au

Citation:
Kennett, B. L. N., E. Saygin, and M. Salmon (2015), Stacking autocorrelograms to map Moho depth with high spatial resolution in southeastern Australia, *Geophys. Res. Lett.*, *42*, 7490–7497, doi:10.1002/2015GL065345.

Received 14 JUL 2015
Accepted 16 AUG 2015
Accepted article online 20 AUG 2015
Published online 29 SEP 2015
Corrected 16 NOV 2015

This article was corrected on 16 NOV 2015. See the end of the full text for details.

Stacking autocorrelograms to map Moho depth with high spatial resolution in southeastern Australia

B. L. N. Kennett[1], E. Saygin[1], and M. Salmon[1]

[1] Research School of Earth Sciences, Australian National University, Canberra, ACT, Australia

Abstract Current estimates of Moho depth in southeastern Australia are based on sparse sampling. The results are augmented with 180 new Moho estimates constructed from spatial stacks of crustal *P* wave reflectivity derived from autocorrelograms at over 750 stations. The spatial stacks of reflectivity are constructed using a Gaussian with half width 0.5°. Picks of the base of crustal reflectivity are made with the aid of the previous Moho model, based on the sparser data, and knowledge of the variation in the character of the crust-mantle boundary across the region. Good ties can be made to previous results from deep reflection profiling. The new information fills in many holes in coverage and provides a Moho map with closer ties to geological provinces. The procedure exploits the continuous records at the stations and just the vertical components and so can be applied to older data for which receiver function techniques cannot be used.

1. Introduction

Since 1993, there have been extensive deployments of portable seismic recorders across southeastern Australia. Initially, relatively sparse broadband stations were deployed [e.g., *Kennett*, 2003], but from 1998 there were also closely spaced networks of short-period recorders in the WOMBAT project [e.g., *Rawlinson et al.*, 2014]. In addition, the national network of permanent broadband stations operated by Geoscience Australia has been steadily augmented. New stations have also recently come into operation through the Australian Seismometers in Schools program that employs broadband sensors [*Balfour et al.*, 2014]. The net result is that over 750 seismic stations have been deployed across southeastern Australia (Figure 1). These stations span from the Precambrian of the South Australian craton to the Phanerozoic Lachlan and New England orogens [*Gray and Foster*, 2004; *Glen*, 2005]. Much of the area such as the Murray Basin has significant sedimentary cover.

Current information on the nature of the crust-mantle transition in southeastern Australia comes from a variety of sources including refraction experiments prior to 1990, receiver function studies, and full-crustal reflection profiling. A detailed model of the depth to Moho for the whole continent was constructed in 2011 [*Kennett et al.*, 2011] and updated in 2013 [*Salmon et al.*, 2013], but with little new information in the southeast. Sampling is sparse across the region, especially across the sedimentary basins. Over a large fraction of the area the current models are interpolated from only a few control points.

Many of the earlier deployments of short-period stations used only vertical component seismometers, so these are not suitable for receiver function analysis. Although it is possible to extract Moho information from receiver functions at higher frequencies in conjunction with surface wave dispersion [*Tkalčić et al.*, 2012], this time-consuming procedure has not been applied across the full suite of stations and can be difficult to apply in areas where reflective sediments cause ringing. *Gorbatov et al.* [2013] have demonstrated that the autocorrelation of the seismic signal and noise from the vertical component at a single seismic station can provide a good estimate of deep crustal and uppermost mantle reflectivity in a wide variety of environments across the Australian continent. The autocorrelation procedure generally works well even with sediments at the surface. Where the Moho is sharp, as in the Basin and Range Province of the United States, such autocorrelations can be used to extract direct estimates of Moho depth [*Tibuleac and von Seggern*, 2012]. However, the transition from crust to mantle across Australia shows highly variable properties, with many broad areas where gradients in seismic wave speed are present, rather than a sharp interface. The result is that the character of the reflectivity at the base of the crust marking the presence of the Moho shows substantial variation

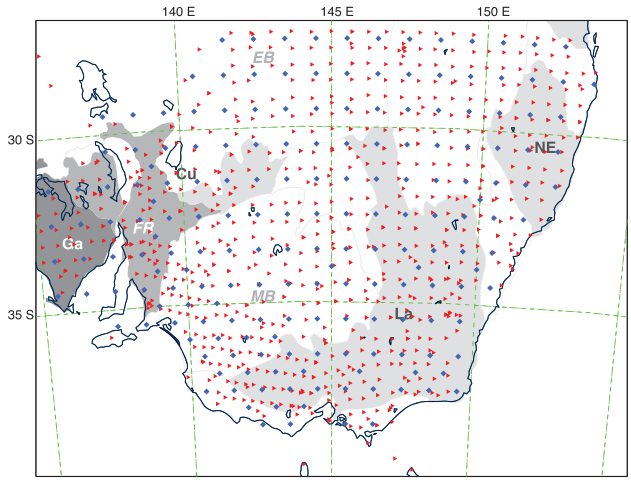

Figure 1. Distribution of seismic stations in southeast Australia indicated by red filled triangles and the locations for which stacked autocorrelograms have been constructed shown with blue diamonds. Major tectonic units are indicated by greytone. Key to marked features: Cu = Curnamona Province, Ga = Gawler Province, La = Lachlan orogen, NE = New England orogen, *FR* = Flinders Ranges, *MB* = Murray Basin, and *EB* = Eromanga Basin.

[*Kennett and Saygin*, 2015]. It is not possible to rely on a single prominent reflector as a marker of the Moho; rather, it is necessary to track the cessation of crustal reflectivity.

Individual station autocorrelograms represent the crustal reflectivity for *P* waves in a passband from 2 to 4 Hz, somewhat lower than used in seismic reflection work. We exploit the consistency between neighboring stations to enhance the coherent portions of the crustal reflectivity using spatial stacks, typically exploiting four to five stations or more. Then, with the aid of an existing Moho model, we can determine improved estimates for the depth to Moho at the stack locations.

We demonstrate this approach by extracting 180 stacked autocorrelograms from the more than 750 seismic stations across mainland southeast Australia and thereby provide new control on Moho structure in regions of hitherto poor sampling. Agreement with independent information is good in regions with good prior control, but some significant changes are required in zones where previous constraints have been lacking.

2. Station Autocorrelograms as Indicator of Reflectivity

For each of the stations across southeast Australia we have constructed autocorrelograms using the procedure described by *Gorbatov et al.* [2013]. The vertical component records from all the various sources of data were resampled to 40 samples per second. Autocorrelograms were then constructed for 6 h time windows of the continuous seismic data using a spectral approach [*Gorbatov et al.*, 2013]. The results from the individual windows were then summed to enhance coherent features and suppress noise. The final traces were filtered with a band pass between 2 and 4 Hz to enhance the reflectivity information below each site. The traces were plotted suppressing lags less than 5 s and then assessed for quality. In a few cases there were indications of periodicity or apparent aliasing artifacts; these stations were discarded. In Figure 1 we plot the locations of the more than 750 stations we have used, situated on the Australian mainland.

The stacked autocorrelograms present the *P* wave reflectivity at individual sites, but because the sites are relatively sparse, it can be hard to link the results to neighboring points. In the supporting information we discuss different displays of the *P* wave reflectivity and in Figure S1 show different representations of the same suite of results for two constant latitude slices across southeast Australia (31.5°S and 33.5°S). In general, we have found the envelope of the autocorrelogram trace to be the most helpful mode of display for recognizing correlations between sparse sites, particularly when used with a greytone variable density representation (see supporting information).

The filtered autocorrelograms provide a representation of the low-frequency *P* wave reflection behavior beneath a site. The crustal response often shows quite rapid spatial variations, with sometimes a distinct basal reflector but often just a fade of reflectivity. At long time lags we still see indications of reflectivity in the

2–4 Hz band. In most locations crustal multiples can be excluded by the timing relations, and so we have evidence for return of reflected energy from the upper part of the mantle lithosphere. These reflective features are not seen in conventional reflection records, which suggests that they correspond to larger-scale features with more gentle impedance variations that would be invisible in the normal reflection regime (> 20 Hz).

Although it is possible to work with the autocorrelograms for individual stations, the relative dense coverage is very suitable for making stacks from nearby stations and thereby enhances coherent features in the crustal reflectivity. This spatial stacking makes the task of estimating the location of the crust-mantle boundary somewhat easier.

2.1. Spatial Stacking Procedure

We extract spatially stacked autocorrelograms across the region on a preassigned grid. For much of the region we have used a regular $1^\circ \times 1^\circ$ grid (Figure 1) with additional stack points introduced in areas where either station density is high or the pattern of stations is inclined to the regular grid.

We combine the autocorrelogram traces with a radial stack $\mathcal{S}$ around each stack point constructed with Gaussian weighting:

$$\mathcal{S}(t) = \frac{\sum_j u_j(t) \exp[-\delta_j^2/\sigma^2]}{\sum_j \exp[-\delta_j^2/\sigma^2]}, \tag{1}$$

where δ_j is the angular distance to the jth station with envelope trace $u_j(t)$ and σ determines the span of the stack. In our applications we have used $\sigma = 0.5^\circ$and truncated the summation in (1) at 3σ where the Gaussian weighting drops below 1.2×10^{-3}. Most of the contribution will come from the zone within 0.9°. Stack traces are only retained if the denominator exceeds 1.5. This procedure stabilizes the envelope traces to provide good sampling in the neighborhood of the stack point, and at most locations the stack denominator exceeds 3.

In Figure 2 we present stacked autocorrelograms for a set of locations that track full-crustal reflection profiles. The stack points are plotted on map strips showing the Moho estimates derived from Moho picks on the reflection records converted to depth using an average velocity of 6 km/s [*Kennett et al.*, 2011]. Below we plot the reflectivity using the stack traces with area fill; the depth axis is based on the 6 km/s conversion. The Moho depth at each point from the model of *Salmon et al.* [2013] is shown with brown markers. An alternative presentation using the trace envelopes with variable density display is shown in Figure S2 in the supporting information. In Figure 2, with each stack record we provide a measure of Moho clarity extracted from the reflection records along the profiles [*Kennett and Saygin*, 2015], where class A is very clear and class D is rather poor. Along the illustrated profiles the reflection Moho is generally moderately clear but in some places is less distinct. As can be seen from Figure 2, the autocorrelation stacks show a similar behavior in the neighborhood of the Moho for much lower frequencies than are employed in the reflection profiling.

The upper strip (Figure 2a) lies mostly in the South Australian craton but crosses the margin into the Phanerozoic at the eastern end. On this strip the Moho lies between 40 and 45 km deep without much variation. The lower profile (Figure 2b) extends from presumed Precambrian material in the Delamerian orogen in the west, under limestone cover, into the Paleozoic Lachlan orogen [*Gray and Foster*, 2004]. Moving from west to east the Moho shallows and then deepens again. In each case there is a close correspondence between the base of crustal reflectivity in the stack traces and the prior Moho estimates. Further, those locations where there is a clear basal reflector, for example, QN1 and QN2, correspond to places where the Moho is well defined in the reflection profiling [cf. *Kennett and Saygin*, 2015, Figure 8]. The changes in Moho depth indicated between QS1 and QS3 match well with the changes in character on the reflection records [*Kennett and Saygin*, 2015, Figure 15].

2.2. Moho Extraction

The good correspondence between the stacked autocorrelograms and Moho structure in regions with good control is encouraging. For much of the southeastern Australian area we do not have direct control on the Moho. Yet we are able to use the Moho model constructed from existing information [*Salmon et al.*, 2013], and knowledge of the character of the crust-mantle transition derived from receiver functions and other sources *Kennett and Saygin* [2015], to guide the assessment of the stack traces.

For each stack location we construct a display similar with those shown in Figure 2 with the envelope of the stacked autocorrelogram and a marker from the 2013 Moho model. We have found it convenient to assemble

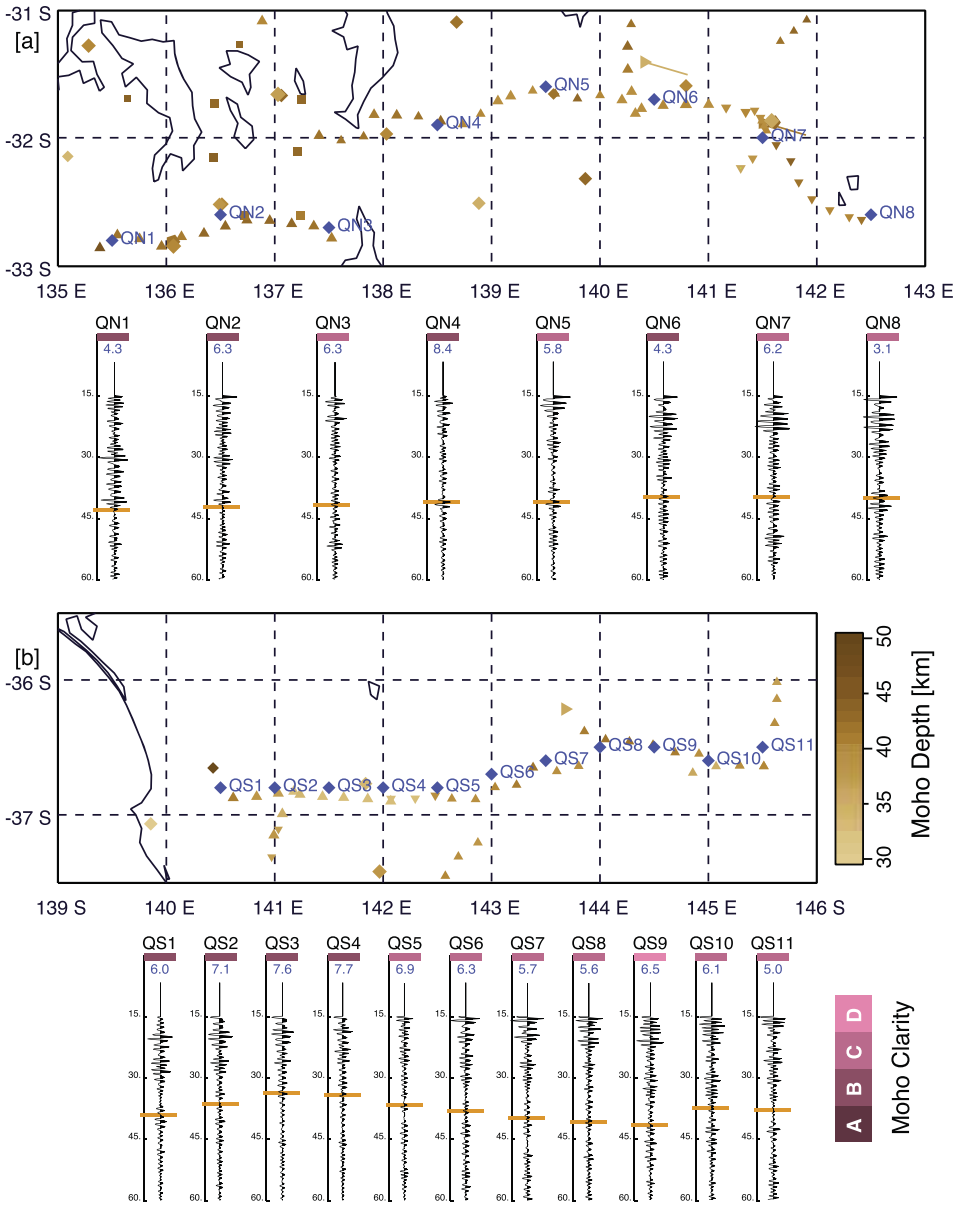

Figure 2. Comparison of stacked autocorrelograms and previous Moho information from full-crustal reflection profiling with area fill on traces. The location of the stack points is shown in map view with the stacks beneath, on which the Moho estimates from the model of *Salmon et al.* [2013] are shown with brown markers. The blue numbers indicate the stack denominator, i.e., the effective number of stations contributing to the stack. (a) Section across the Gawler and Curnamona Provinces of the South Australian craton. (b) Section from the Delamerian to the Lachlan orogen (Phanerozoic). For each stack point the measure of Moho clarity taken from the reflection records is indicated by a colored bar.

the stack traces into constant latitude or constant longitude strips and to then make assessments of the base of crustal reflectivity as an indicator of the Moho. The use of the ensemble of traces helps to pick up systematic variations in reflectivity character with position but does not preclude sharp changes in Moho depth between sites a degree apart. Working separately with latitude and longitude displays provides different perceptions of the individual traces, but we have found that the assessment of Moho location is very consistent between the two representations, rarely exceeding 0.5 km.

In making the assessment of Moho depth we have to take into account the full range of information on the nature of the crust-mantle transition using information, where available, from prior reflection profiling

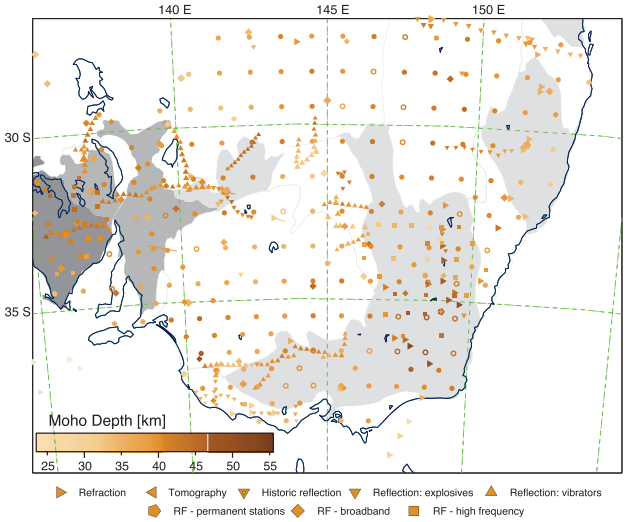

Figure 3. Comparison of Moho depth estimates from stacked autocorrelograms indicated by circles with prior information from a variety of sources [*Salmon et al.*, 2013], superimposed on the tectonic features from Figure 1. The clarity of the Moho varies across the region because in many locations the crust-mantle transition is gradational. Instances of weak direct Moho indicators for the stacked autocorrelograms are shown with open circles.

or receiver function results. The picks are based on an estimate of the base of crustal reflectivity in the autocorrelogram stacks rather than necessarily a specific basal reflector. Where there is a gradient in properties at the base of the crust, the reflectivity tends to fade, so the uncertainty in the Moho pick is larger.

The Moho picks from the autocorrelogram results are for two-way reflection time from the surface and so need to be converted to depth for integration with other estimates. We have used the same time to depth conversion of an average 6 km/s for the stacked autocorrelograms as previously used for the full-scale reflection profiling. This procedure has been calibrated in a number of places around the continent by comparison of high-quality receiver function results with reflection records displaying a clear Moho and is unlikely to produce more than 1 km error for a Moho depth of 40 km (i.e., 2.5%). In regions with thick sedimentary cover the average velocity might be a little too high, and so the Moho depth would be overestimated. However, even in the extensive sediments of the Murray Basin, the thickness rarely exceeds 500 m [*Brown and Stephenson*, 1991], and hence, such corrections will be small for the area studied. Because we are working with a band pass of 2–4 Hz, the time picks are unlikely to be better than 0.125 s which introduces a depth error on the order of 0.5 km.

In Figure 3 we display the full set of Moho estimates from the stacked autocorrelograms, together with the previously available Moho results from a range of different data. Locations where the direct Moho indicator is weak in the stacked autocorrelograms are shown with open circles. These locations occur where previous information suggests the presence of a gradient in properties at the base of the crust. In particular, we have a strong concentration with the Lachlan Fold Belt where both refraction experiments and receiver function studies indicate a gradational transition from crust to mantle [cf. *Kennett et al.*, 2011].

The correspondence of the new estimates from the stacked autocorrelograms with prior results is good. There are, however, a few places where we see some discrepancies. These are mostly with receiver function results, where it appears that a prominent discontinuity may have been picked somewhat shallower than the true base of the crust, e.g., at the top of a transitional zone (as seen in Central Australia).

The use of the stacked autocorrelograms significantly increases Moho information into regions of cover with little prior information, such as the Murray Basin and the southern Eromanga Basin in the north of the region. The new results show clearly horizontal gradients in structure, e.g., thickening of the crust to the north near 29°S, 144°E seen from reflection profiling. Other features can now be better mapped with the expanded spatial coverage as discussed in the next section.

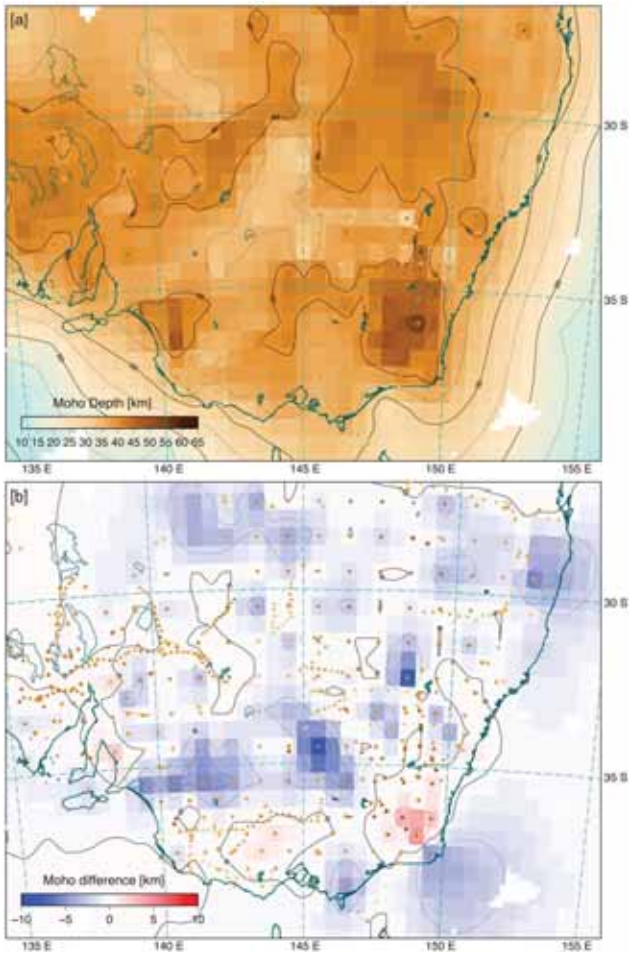

Figure 4. (a) Moho depth map for southeastern Australia, incorporating the results from the stacked autocorrelograms. (b) Difference map for Moho depth from the 2013 compilation [*Salmon et al.*, 2013], with blue colors where the new estimates are deeper. In each panel the different classes of Moho information are plotted color coded by depth with the same conventions as in Figure 3.

3. Discussion and Conclusions

In Figure 4a we display the map of Moho depth for the southeastern corner of mainland Australia, with the stacked autocorrelogram results added to those employed in the compilation of *Salmon et al.* [2013]. The approach used for the construction of the map follows that described by *Kennett et al.* [2011], which was also used by *Salmon et al.* [2013]. The interpolation tools from the Generic Mapping Tools package [*Wessel and Smith*, 1998] are employed in a conservative approach targeted at 0.5° resolution across the continent. In each 0.5 × 0.5° cell the weighted mean Moho depth from all estimates in the cell is constructed. Individual data points are weighted using an assessment of the data reliability [*Kennett et al.*, 2011]. We have included the stacked autocorrelogram results with the relatively low weighting of 0.4 to allow for the depth conversion and picking errors. We thereby avoid dominating other depth estimates where these are available. In many cells the autocorrelogram results are the only ones available and so will play an important role in defining the surface. The weighted means for each cell are interpolated with a single surface, using a gridding algorithm with an adjustable tension continuous curvature [*Smith and Wessel*, 1990]. In order to allow for steep Moho topography, the tension factor is set to 0.45.

Although the surface is continuous, we display the results in Figure 4 with pixelation for each 0.5 × 0.5° cell and superimpose the Moho depth estimates from Figure 3. The success of the procedure for representing the Moho is attested by the fact that very few of the individual points are at all visible.

Figure 4b shows the difference surface between the new Moho depth model shown in Figure 4a and the results of *Salmon et al.* [2013]. Deeper Moho depth estimates in the current model are negative, indicated by blue tones. Shallower estimates are positive and appear in red. Most of the changes from the introduction of the stacked autocorrelogram results have resulted in a slight deepening of the Moho, particularly in regions with hitherto limited control where the model of *Salmon et al.* [2013] depended on interpolation from distant points.

The addition of the extensive new direct information on Moho depth gives a distribution with a clearer tie to geological structures. Near 33°S, 140°E the zone of thickened crust revealed in reflection profiling [see *Kennett and Saygin*, 2015, Figure 15], which ties with a single nearby receiver function result [*Fontaine et al.*, 2013], can now be seen to have at least 1.5° extent. It is likely that this feature is associated with the edge of the South Australian craton, modified in the Delamerian orogen [*Foden et al.*, 2006]. Farther east the spatial extent of the zone of rather thick crust, with a gradational base, in the eastern part of the Lachlan orogen (near 37°S, 148°E) is now better spatially defined. Beneath the Murray Basin, the new results suggest a sightly thicker crust than in early models, and a similar trend is apparent in the southern part of the Eromanga Basin where previously there were only a few scattered constraints from earlier studies. The region of the New England orogen [*Glen*, 2005] now appears as a more distinct entity, separated from some thicker crust (>40 km thick) in the northern Lachlan, under cover.

The exploitation of estimates of crustal reflectivity extracted from vertical component seismic records has allowed a uniform treatment of data from a wide variety of seismic stations. With enhancement of the crustal signals using a Gaussian spatial stack, over 180 new estimates of the depth to Moho across southeastern Australia have been generated, with direct results provided for the first time in many areas under cover. The construction of the station autocorrelograms and the subsequent stacking procedures can be automated, but careful inspection of the results is desirable to avoid the introduction of spurious information.

Even in a region with a very variable character of the transition between crust and mantle such as southeastern Australia, the stacked autocorrelograms provide a good representation of the reflectivity in the lower part of the crust and into the upper mantle. Interpretation of the choice of Moho at each stack site is aided by marking the expected location from a prior model, together with any available information on the character of the expected crust-mantle transition [*Kennett et al.*, 2011; *Kennett and Saygin*, 2015]. Unless the expected Moho is very sharp, it will be very hard to automate the pick. But multiple picks using displays with different directions of cut through the data volume of stacked autocorrelograms (e.g., in latitude and longitude) can be used to refine the results.

The autocorrelogram results provide indications of noticeable reflectivity well beneath the base of the crust for the 2–4 Hz frequency band we have employed (cf. Figure 2). This suggests that the apparent transparency of the upper mantle in deep seismic reflection profiles may be a function of the wavelengths employed. Rather than sharp interfaces, it would appear that these lower frequency reflections are returned from gradients in impedance over length scales of a few hundred meters.

Acknowledgments

The data for the Australian permanent stations were accessed from the IRIS Data Management Center. The portable experiments have been supported by a variety of funding sources including the Australian National University, the Australian Research Council, and AuScope. These data have been taken from the archive maintained at the Research School of Earth Sciences, Australian National University to which access can be arranged on request. We would like to extend thanks to the members of RSES, ANU who have deployed the extensive set of portable seismic recorders across the Australian continent that have been exploited in this study. ObsPy [*Beyreuther et al.*, 2010] was used for the file format conversions and data management.

The Editor thanks Alan Levander and an anonymous reviewer for their assistance in evaluating this paper.

References

Balfour, N. J., M. Salmon, and M. Sambridge (2014), The Australian Seismometers in Schools network: Education, outreach, research, and monitoring, *Seismol. Res. Lett.*, *85*, 1063–1068.

Beyreuther, M., R. Barsch, L. Krischer, T. Megies, Y. Behr, and J. Wassermann (2010), ObsPy: A Python toolbox for seismology, *Seismol. Res. Lett.*, *81*, 530–533.

Brown, C. M., and A. E Stephenson (1991), *Geology of the Murray Basin, Southeastern Australia*, Scale 1:500000. Bulletin 235, Bureau of Mineral Resources, Geology and Geophysics, Canberra.

Foden, J., M. A. Elburg, P. B. Smith, J. Dougherty-Page, and A. Burtt (2006), The timing and duration of the Delamerian orogeny: Correlation with the Ross orogen and implications for Gondwana assembly, *J. Geol.*, *114*, 189–210.

Fontaine, F., H. Tkalčić, and B. L. N. Kennett (2013), Imaging crustal structure variation across southeastern Australia, *Tectonophysics*, *582*, 112–125.

Gorbatov, A., B. L. N. Kennett, and E. Saygin (2013), Crustal properties from seismic station autocorrelograms, *Geophys. J. Int.*, *192*, 861–870.

Glen, R. A. (2005), The Tasmanides of eastern Australia, in *Terrane Processes at the Margins of Gondwana*, edited by A. P. M. Vaughan, P. T. Leat, and R. J. Pankhurst, pp. 23–96, Geol. Soc., London, U. K.

Gray, D. R., and R. A. Foster (2004), Tectonic evolution of the Lachlan Orogen, southeast Australia: Historical review, data synthesis and modern perspectives, *Austral. J. Earth Sci.*, *51*, 773–817.

Kennett, B. L. N. (2003), Seismic Structure in the mantle beneath Australia, in *The Evolution and Dynamics of the Australian Plate*, vol. 372, edited by D. Müller and R. Hillis, pp. 7–23, Geological Soc. of Australia Spec. Publ. 22 and Geol. Soc. Am., Sydney, Australia.

Kennett, B. L. N., and E. Saygin (2015), The nature of the Moho in Australia from reflection profiling: A review, *GeoResJ*, *5*, 74–91.

Kennett, B. L. N., M. Salmon, E. Saygin, and AusMoho Working Group (2011), AusMoho: The variation in Moho depth in Australia, *Geophys. J. Int.*, *187*, 946–958.

Salmon, M., B. L. N. Kennett, T. Stern, and A. R. A. Aitken (2013), The Moho in Australia and New Zealand, *Tectonophysics*, *609*, 288–298, doi:10.1016/j.tecto.2012.07.009.
Smith, W. H. F., and P. Wessel (1990), Gridding with continuous curvature splines in tension, *Geophysics*, *55*, 293–305.
Rawlinson, N., M. Salmon, and B. L. N. Kennett (2014), Transportable seismic array tomography in southeast Australia: Illuminating the transition from Proterozoic to Phanerozoic lithosphere, *Lithos*, *189*, 65–76.
Tibuleac, I. M., and D. von Seggern (2012), Crust-mantle boundary reflectors in Nevada from ambient seismic noise autocorrelations, *Geophys. J. Int.*, *189*, 493–500.
Tkalčić, H., N. Rawlinson, P. Arroucau, A. Kumar, and B. L. N. Kennett (2012), Multi-step modelling of receiver-based seismic and ambient noise data from WOMBAT array: Crustal structure beneath southeast Australia, *Geophys. J. Int.*, *189*, 1681–1700.
Wessel, P., and W. H. F. Smith (1998), New, improved version of Generic Mapping Tools released, *Eos Trans. AGU*, *79*, 579.

Erratum

In the originally published version of this article, the supporting information file was omitted. The file has since been included, and this version may be considered the authoritative version of record.